 doi:10.20944/preprints201610.0058.v1

Communication

Local Electrical Response in Alkaline-Doped Electrodeposited $CuInSe_2$/Cu Films

Liliana E. Arvizu-Rodríguez [1], Javier A. Barón-Miranda [2], Octavio Calzadilla [3], Jose L. Fernandez-Muñoz [4], Cesia Guarneros-Aguilar [5], Fabio F. Chalé-Lara [2], Ulises Páramo-García [1] and Felipe Caballero-Briones [2,*]

[1] División de Estudios de Posgrado e Investigación, Instituto Tecnológico de Cd. Madero, 89460 Cd Madero, México; liliarvizurdz@gmail.com (L.E.A.-R.); uparamo@itcm.edu.mx (U.P.-G.)
[2] Instituto Politécnico Nacional, Materiales y Tecnologías para Energía, Salud y Medioambiente (GESMAT), CICATA Altamira. Km.14.5 Carretera Tampico-Puerto Industrial, 89600 Altamira, México; armandobaron1150@gmail.com (J.A.B.-M.); fchale@ipn.mx (F.F.C.-L.)
[3] Facultad de Física, Universidad de La Habana, San Lázaro y L, Vedado, 10400 La Habana, Cuba; calza@fisica.uh.cu
[4] Instituto Politécnico Nacional, CICATA Legaria. Calzada Legaria 396 Col. Irrigación, 11500 CdMx, México; jlfernandez@ipn.mx.
[5] CONACYT-Instituto Politécnico Nacional, GESMAT-CICATA Altamira, 07738 Ciudad de Mexico, Mexico; cguarnerosag@conacyt.mx
* Correspondence: fcaballero@ipn.mx; Tel.: +52-55-57-296300 (ext. 87508)

Abstract: The local electrical response in alkaline-doped $CuInSe_2$ films prepared by single step electrodeposition onto Cu substrates was studied by current sensing atomic force microscopy. The CIS films were prepared from single baths containing the dopant ions (Li, Na, K or Cs) and were studied by X-ray diffraction, scanning electron microscopy, energy dispersive X-ray spectroscopy and photocurrent response. Increased crystallinity and surface texturing as the ion size increases was observed as well as enhanced photocurrent response in Cs doped CIS. Li and Na doped films have larger conductivity than the undoped film while the K and Cs doped samples display shorter currents and the current images indicate strong charge accumulation in the K and Cs doped films forming surface capacitors. Corrected CAFM IV curves were adjusted with Shockley equation.

Keywords: $CuInSe_2$ electrodeposition; alkaline doping; current sensing atomic force microscopy

1. Introduction

$CuInSe_2$ (CIS) is a p-type semiconductor with interest for solar cells [1], photo catalysis [2] and water splitting [3]. The electrical properties of CIS depend on its defect chemistry [4]. With respect to alkaline doping, Na incorporation after deposition leads to enhanced current transport, attributed to Se vacancy passivation [5], but also to introduction of acceptor defects, elimination of InCu donors or elimination of defects at grain boundaries [6]; when incorporated during growth, Na affects Cu homogeneity on a microscopic level, leading to lower charge carrier mobilities [7]. In the case of Li, small contribution to the valence or conduction band states was found although an increase in the band gap was attributed to effects on Se p-orbitals due to Li ionicity [8]. For K doping in $Cu(In,Ga)Se_2$ a reduced minority carrier lifetime, poorer and temperature dependent collection of photogenerated charge carriers was observed [6]. Finally, in a study of anodic p-Cu_2O films doped with Li, Na, K and Cs [9] a shift of the acceptor level position together with increase of the carrier density and electrical conductivity and a reduction in the photocurrent response with the dopant ion size was observed. First-principles calculations indicate a net attractive interaction for Li–O bonds, a

 doi:10.20944/preprints201610.0058.v1

slightly repulsive interaction for Na–O, and a net repulsive interaction for K–O and Cs–O respectively.

On the other hand, current sensing atomic force microscopy is a powerful tool to observe the local electrical properties and electrically active sites at grain and grain boundaries. Its usefulness has been tested in many photovoltaic devices, for example in assessing photoactivity in $CuInSe_2$/Au nanowire arrays [10] and to study the current routes in polycrystalline CIS and CIGS [11]. However, the exploiting of CAFM-IV curves in CIS and doped CIS has been scarcely done. CAFM-IV curves carry additional information on the surface states and grain boundaries and physical information such as barrier height, series resistance and ideality factor of the diode-like junction between tip and sample that can be modelled with the appropriate model [12]. In this work, $CuInSe_2$/Cu films were prepared by electrodeposition and Li, K, Na or Cs ions were added during the growth. The nanoelectrical and photocurrent response was studied and interpreted in terms of the dopant effects on crystalline and electronic structure.

2. Materials and Methods

Electrodeposition of $CuInSe_2$ films was done at pH 2 onto chemically polished, single-sided PC boards using an Autolab 302 station with the Cu-cladded board as working electrode, Pt gauze as counter electrode and a Ag/AgCl reference electrode [13]. The Cu^{2+}:Se^{4+}:In^{3+} ratio in the bath was set to 1:1:2. The dopant solutions of 0.1 M LiOH, NaOH, KOH, CsOH were added in proper volume to achieve a 1:10 dopant/Cu^{2+} ratio in the bath. The substrates were introduced into the electrolyte 2 min before applying potential to form a reddish Cu_2Se buffer layer, this layer has been found as necessary to ensure adhesion; then the potential was swept from OCP to -1500 mV at 5 mVs^{-1} and maintained during 15 min. Finally, the samples were rinsed with deionized water and dry under N_2 stream. X-ray diffractograms were acquired in a Bruker D8 Advance in the Bragg-Brentano geometry using CuKα radiation. Photocurrent response was recorded in the constant wave mode using 0.1 M $NaNO_3$ as electrolyte, sweeping the potential at a 5 mVs^{-1} rate [14]. Illumination was done using a 75 W quartz tungsten halogen lamp onto a 1.2 cm^2 area. Scanning electron microcopy and energy dispersive X-ray spectroscopy (EDS) were done in an EDAX/Quanta microscope operating at 20 kV. Current sensing atomic force microscopy (CAFM) was done in a Dimension microscope (Veeco) microscope using solid Pt/Ir bend wire tips (RMN 25Pt300B, Bruker). Topographic and current images were acquired at +100 and -100 mV bias and the IV curves were recorded after imaging a conductive site; the potential was applied to the sample holder while keeping tip grounded. Three points in the sample were imaged and each reported curve is the average of at least 50 measurements.

3. Results and Discussion

3.1. Morphology, Composition and Structural Characterization

Figure 1 presents the SEM images at two different magnifications of the prepared CIS and alkaline-doped CIS films and the atomic composition at the side of the SEM images. EDS spectra were obtained at the grain surface, the grain edges and in the apparent bottom of the images to assess the growth dynamics. Cu, In, Se and O was detected in all the films and Cu large concentration arises from substrate.

Preprints (www.preprints.org) | NOT PEER-REVIEWED | Posted: 14 October 2016 doi:10.20944/preprints201610.0058.v1

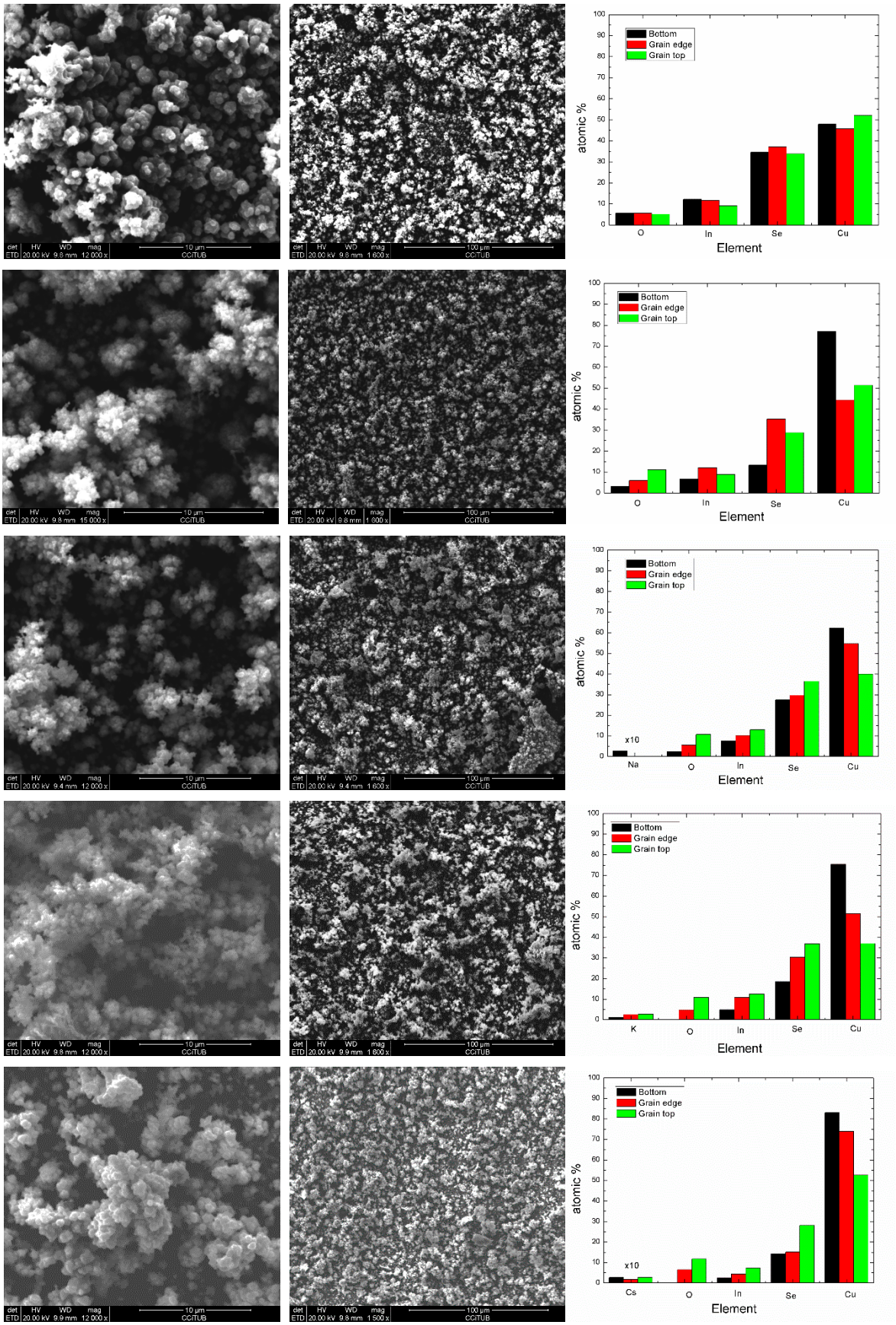

Figure 1. Left and center columns. SEM micrographs obtained at 12000 X and 1500 X; right column: EDS data of the CIS, CIS:Li, CIS:Na, CIS:K and CIS:Cs films (from top to bottom) obtained at the image apparent bottom (black bar), grain edge (red bar) and grain top (green bar).

Preprints (www.preprints.org) | NOT PEER-REVIEWED | Posted: 14 October 2016 doi:10.20944/preprints201610.0058.v1

SEM images indicate an island type of growth with continuous grain formation and no coalescence. Li, Na and K doped films are porous, suggesting H_2 evolution. CIS and CIS:Cs films consist in defined grains, with rounded (CIS) and faceted (CIS:Cs) aspect respectively.

Undoped CIS film composition is almost constant thru the film depth as the analysis of the composition measured at the different parts of the images indicate. Selenium excess with respect to In:Se 1:2 ratio is due to the Cu_2Se buffer layer. Detectable alkaline ions (Na, K and Cs) maximum contents were Na 0.25 at%, K 2.80%, and Cs 0.28% respectively. The higher amount of K is intriguing because its Pauling ion size (133 pm) exceeds that of Cu (96 pm) [9]. The explanation could be that K is not getting incorporated into the CIS lattice as expected but segregates to grain boundaries [6]. In the case of Na-doped CIS, Na was only detected at the film bottom in contrast with K and Cs that were detected in all the film. Oxygen concentration increases in all the films from the bottom to the top, except for the undoped films, suggesting progressive oxidation during film growth, promoted by the alkaline ions [5] and confirming Li incorporation to the film.

Figure 2 shows the X-ray difractograms of the deposited films, separated into A and B ranges for an easier discussion of the observed diffraction peaks.

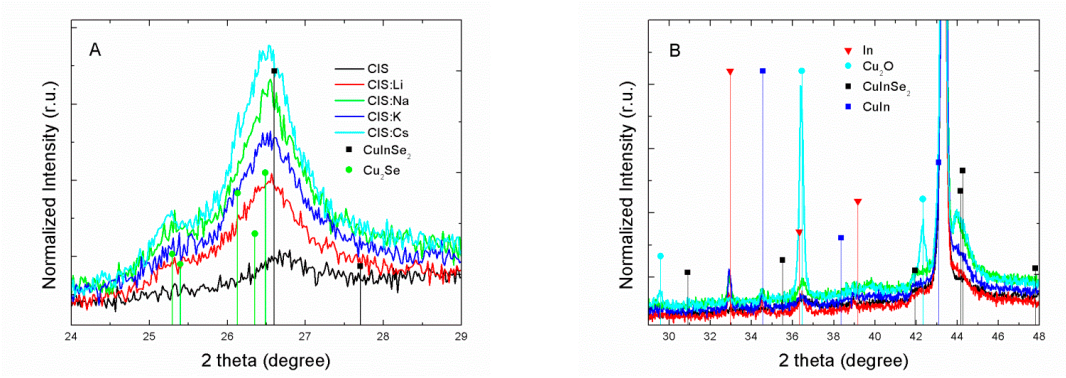

(**a**) (**b**)

Figure 2. X-ray diffractograms of the prepared films.

Figure 2A displays the XRD in the region 2theta 24-29°, around the main peak of tetragonal CIS. In this region, the patterns present a wide peak associated to tetragonal CIS near 26° as well as a shoulder associated with triclinic Cu_2Se at 25.3°. Cu_2Se presence arises from the buffer layer deposited before CIS growth but also could be deposited during the growth [13]. A progressive increase of the relative intensity of the main CIS peak is observed from the undoped<Li<Na<Cs suggesting increase of film thickness. The peak intensity in CIS:K shows a decrease with respect to CIS:Na, that could be attributable to the reported influence of K on elemental interdiffusion when added during growth [6]. On the other hand, the XRDs presented in Figure 2B display peaks corresponding to Cu_2O at 29.5°, 36.4° and 42.3° respectively in all the patterns but particularly evident in the Cs doped sample; elementary In is particularly strong in the K doped sample and a small peak corresponding to CuIn at 34.5° displays also in the K sample, both could be attributed to a less complete reaction because the above mentioned K-dependent hindering of elementary diffusion. The presence of Cu_2O would arise from early oxide formed before deposition, but in the case of the Cs-doped film is evident that is mostly formed during growth. In a previous report [9] alkaline doped Cu_2O films were prepared by anodization. In that report the Cu substrate was first

Preprints (www.preprints.org) | NOT PEER-REVIEWED | Posted: 14 October 2016 doi:10.20944/preprints201610.0058.v1

cathodized in order to "load" it with the alkaline ions, before proceed to anodization. It was observed that film growth was hindered upon strong Cs absorption onto the substrate. In the present report, au contraire, film cathodic deposition seems to be enhanced when Cs is added during growth. According the early work of R. Notoya [15] the effect could be attributed to Cs^+ adsorption that would lead to a local increase in pH, thus increasing the H_2 evolution overpotential, making more efficient the deposition current therefore film thickness. The increase in Cu_2O formation could be explained also by this increase in local pH, where the source of oxygen would be the decomposed water onto the adsorbed Cs^+ [15]. Additionally, it is known that alkali metals have a catalytic effect on semiconductor oxidation as they induce polarization in O_2 molecule leading to easily dissociable O_2^- [5], the effect in the electrolyte solution is the above described increase in pH upon alkali-catalyzed water dissociation.

3.2. Photocurrent Response

Figure 3 presents the photocurrent response of the films in front of a $NaNO_3$ electrolyte during a continuous potential sweep from OCP to -250 mV vs SSC.

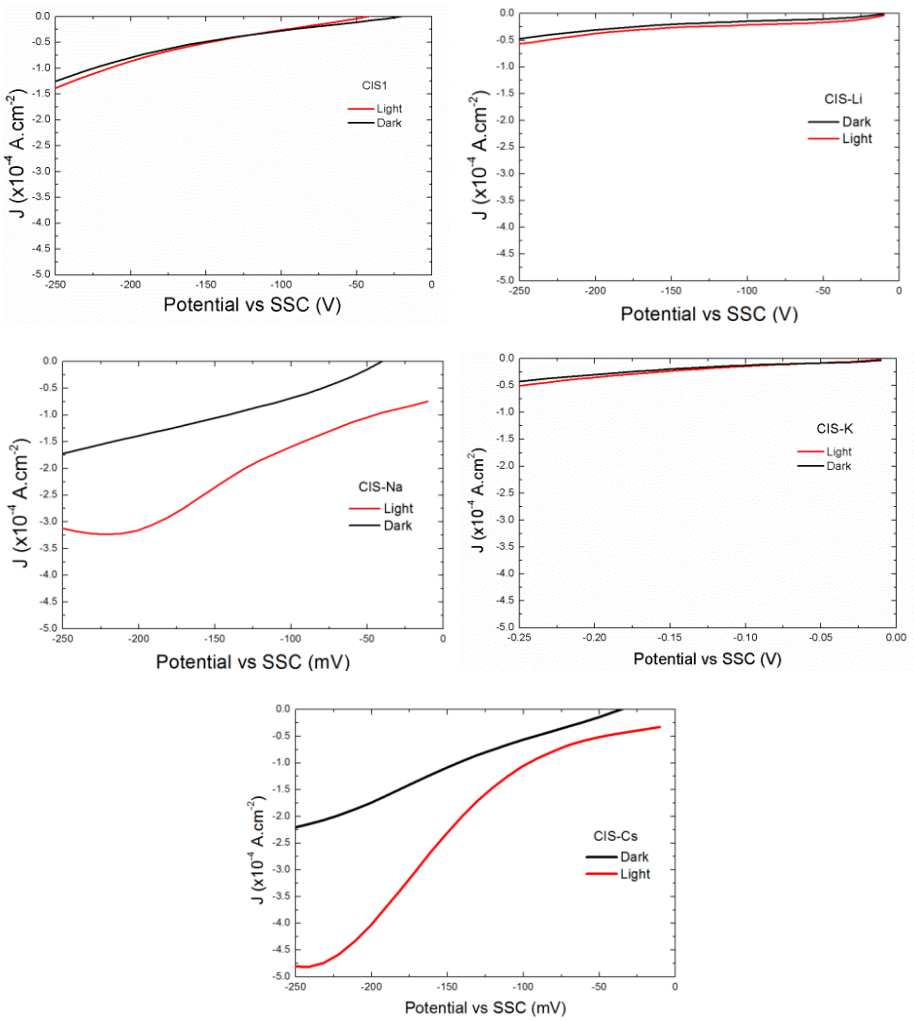

Figure 3. Photocurrent response of the alkaline doped CIS films (a) Undoped, (b) CIS:Li, (c) CIS:Na (d) CIS:K and (e) CIS:Cs.

Preprints (www.preprints.org) | NOT PEER-REVIEWED | Posted: 14 October 2016 doi:10.20944/preprints201610.0058.v1

The films present almost any noticeable photocurrent response (PCR) except the Na-doped and the Cs-doped films. The lack of PCR can be attributed to the presence of the deleterious Cu_2Se phase within the films as well as metallic phases such as In and CuIn, particularly in the K-doped film. On the other hand, the increase in the photocurrent response in the films doped with Na and Cs could be due to the catalyzed oxidation of the semiconductor surface [5] that lead to Se vacancy neutralization, a well-known recombination center in CI(G)S and the formation of p-Cu_2O. Therefore the effect of Na and Cs will overcome the effect of the deleterious Cu_2Se phase through progressive $(Cu_2Se)_{1-x}(Cu_2O)_x$ formation in the Cu_2Se surface, as the relative intensities of the Cu_2O and Cu_2Se/CIS peaks in the Cs- and Na-doped films indicate. In the case of K, the observed formation of metallic phases within the film would deteriorate any photocurrent response, but also there are reports that mention that *au contraire* to Na-doping which beneficial effect has been related to V_{Cu} capture and thus Cu mass transport [16], K creates electron traps, particularly on Cu-poor CIS films [17] that would also deteriorate the photocurrent response, as actually observed.

3.3. Electrical Characterization by CAFM

Figure 4 presents the CAFM images of the films, acquired at +100 mV. The Figure shows the over imposed topography and electrical signals. The scheme on the top-left section indicates the expected current flux at the employed bias applying the potential to the sample: holes from the film will flow to the tip. The image corresponding to the undoped film displays current flowing uniformly mostly through the grain boundaries. Conversely, the CIS:Li, CIS:Na and CIS:K display current patches accumulated in some grain junctions, without an uniform distribution, although some conduction through the GBs can be observed. Finally, the image of the CIS:Cs film displays accumulated charges onto the grain surfaces, rather than at grain boundaries. The observations indicate that doping addition during film growth originates non-uniform dopant distribution, although the effect of doping on the conductance upon voltage biasing will be discussed below. In the case of Cs-doped CIS the observations are consistent with the above discussed Cs^+ adsorption and further formation of Cu_2O on the top of the grains.

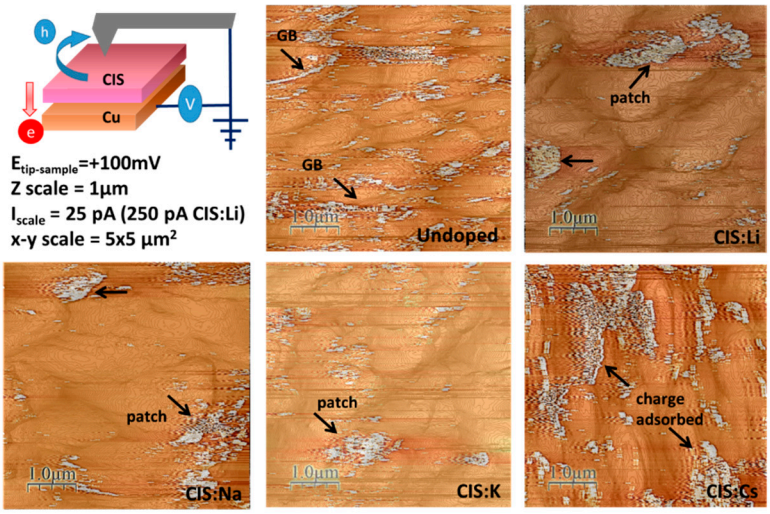

Figure 4. Top left: scheme of the setup of the CAFM measurement and summary of experimental conditions and image characteristics. Images: over imposed topography and current images of the films. Arrows indicate current flow paths.

Preprints (www.preprints.org) | NOT PEER-REVIEWED | Posted: 14 October 2016 doi:10.20944/preprints201610.0058.v1

Figure 5 presents the averaged and corrected IV curves, where the displayed curves arise from at least 50 curves acquired in three different locations for each sample. The x-y displacements were corrected for the sake of curve fitting from (0,0). The non-corrected curves are presented in the Supplementary Information (Figures S1-S5). In Figure 5, the curve of the undoped film displays a rectifying behavior in a bias range 0-750 mV indicating a short space charge layer, compared with the doped films, possibly due to charged defects and foreign phases. The curve corresponding to the Li-doped film presents a rectifying section up to 1700 mV. Another noticeable feature is the large tip-sample current range (up to 12.5 nA) with respect to the undoped film (ca. 100 pA). The higher conductance of the CIS:Li is possible due to the substitutional incorporation of Li CIS lattice, leading to increase in carrier concentration [18]. The I-V curve of the Na-doped film shows an extended, well-defined rectifying behavior up to 3000 mV and current injection from the contacts above 3000 mV. The current level (12.5 nA) is similar to that of CIS:Li. The literature reports that Na-doping is beneficial for $CuInSe_2$ by creating electrically benign defects that are not electron traps [5,6]. The I-V curve of the K-doped CIS film presents very similar characteristics as that of undoped CIS, i.e. rectifying behavior up to 750 mV but smaller current response, ca. 10 pA vs 100 pA in the CIS sample, confirming the deleterious effect of K in the electrical behavior, also reflected in th photocurrent response. Finally, the I-V curve of the Cs-doped CIS film shows a rectifying behavior up to 1500 mV. Figures S4 and S5 show that both IVs from CIS:K and CIS:Cs display large hysteresis as well as x-y displacement. The behavior confirms the charge accumulation observed in the CAFM images originating the formation of surface capacitors. However, as discussed before, only Cs-doping seems to be beneficial for the photocurrent response although a deeper investigation of Cs incorporation on the electronic properties is needed.

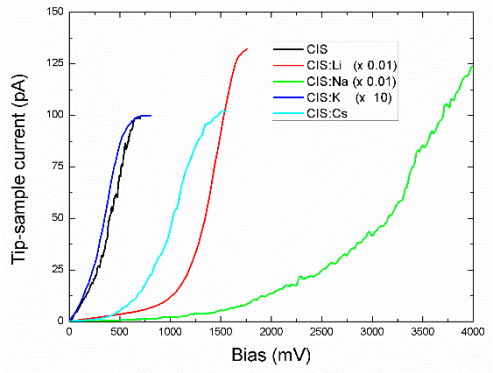

Figure 5. Averaged and corrected CAFM IV curves in the forward sweep and first quadrant of the undoped CIS and alkaline doped CIS films.

The IV curves were fitted with the Shockley equation.

$$I_D = I_S\left(e^{\frac{V_D}{nV_T}} - 1\right) \quad (1)$$

Where Is inverse saturation current, V_D the forward bias applied thru the diode, n the ideality factor and V_T the thermal dependent voltage determined by kT/q where k is the Boltzmann constant, T the room temperature and q the elementary electron charge. The fitting parameters are presented in Table 1. No particular tendency related with ion sizes is observed because the large dispersion in the IV curves (see Figures S1-S5 in Supplementary information); however, the large values of n indicate

 doi:10.20944/preprints201610.0058.v1

prevalence of tunneling conduction mechanisms rather than thermoionic emission caused by the uneven distribution of dopants incorporated during film growth. Future work is intended to "load" the dopants on the Cu substrate before film growth as reported in [9], although the effect of Cu_2O formation must be assessed too as it has been suggested it could have a beneficial effect in back contacts in CdTe solar cells.

Table 1. Fitting parameters

Sample	A	Is	n
CIS	204	21.7+0.7	11.40
CIS:Li	708	490+30	9.78
CIS:Na	60	1079+60	16.24
CIS:K	1022	2.41+0.09	22.5
CIS:Cs	1085	5.4+0.2	10.45

4. Conclusions

Alkaline (Li, Na, K and Cs) doped $CuInSe_2$ films were growth by electrodeposition in a single bath. Ion size influences the photocurrent as well as the dark local current by substitutional incorporation such as Li or by surface accumulation in the case of Cs. The reported beneficial effect of sodium upon photocurrent response was not observed because ion doping was done during the film growth, thus distribution is uneven. From CAFM measurements the local charge segregation was observed as well as the rectifying behavior. Cesium doping appears to be very attractive for future applications such as photocatalytics or photovoltaics because the enlargement of the space charge layer by the creation of a capacitive interface.

Acknowledgments: Financial support from SIP20161804/0291 project as well as by EDI and SIBE grants (F.C.-B., J.L.F.-M., F.F.C.-L.) is acknowledged. C.G.-A. is financed by Cátedras CONACYT 1061-Project. L.A.-R. and J.A.B.-M. acknowledge CONACYT scholarships. O.C. thanks SIP20161804 visiting professor support. Just as the TNM-5534.15-P project (U.P.-G). CCiTUB and specially Dr. Jordi Diaz and Dr. Eva Prats are acknowledged for instrumental facilities and technical support (SEM/EDS and Nano units).

Author Contributions: L.A.-R. performed film growth; J.A.B.-M. ran CAFM and SEM measurements; O.C. simulated and fitted IV curves; J.L.F.-M. measured photocurrent response; C.G.-A. ran XRD measurements; F.F.C-L. did data analysis. U.P.-G. and F.C.-B. conceived the experiments and wrote the paper.

Conflicts of Interest: The authors declare no conflict of interest. The founding sponsors had no role in the design of the study; in the collection, analyses, or interpretation of data; in the writing of the manuscript, and in the decision to publish the results.

References

1. Shrestha, S. Photovoltaics literature survey. *Prog. Photov: Res. Appl*. **2014**, 22, 502–504, DOI: 10.1002/pip.2492
2. Zeming Wu, Xi Tong, Pengtao Sheng, Weili Li, Xuehua Yin, Jianmei Zou, Qingyun Cai. Fabrication of high-performance $CuInSe_2$ nanocrystals-modified TiO_2 NTs for photocatalytic degradation applications. *Appl. Surf. Sci.* **2015**, 351, 309–315, http://dx.doi.org/10.1016/j.apsusc.2015.05.147
3. Wilman Septina, Gunawan, Shigeru Ikeda, Takashi Harada, Masanobu Higashi, Ryu Abe and Michio Matsumura. Photosplitting of Water from Wide-Gap Cu(In, Ga)S_2 Thin Films Modified with a CdS Layer and Pt Nanoparticles for a High-Onset-Potential Photocathode. *J. Phys. Chem. C*, **2015**, 119(16), DOI: 10.1021/acs.jpcc.5b02068
4. Guillemoles, J.F. The puzzle of Cu(In,Ga)Se_2 (CIGS) solar cells stability. *Thin Solid Films* **2002**, 403-404, 405–409, http://dx.doi.org/10.1016/S0040-6090(01)01519-X

5. Kronik, L.; Cahen D. and Werner-Schock, H. Effects of Sodium on Polycrystalline Cu(In,Ga)Se_2 and Its Solar Cell Performance. *ACS Adv. Mater.* **1998**, 10, 31-36, DOI: 10.1002/(SICI)1521-4095(199801)10:1<31::AID-ADMA31>3.0.CO;2-3
6. Pianezzi, F.; Reinhard, P.; Chirila, A.; Nishiwaki, S.; Bissig, B.; Buecheler, S. and Tiwari, A. N. Defect formation in Cu(In,Ga)Se_2 thin films due to the presence of potassium during growth by low temperature co-evaporation process. *J. Appl. Phys.*, **2013**, 114, 194508, http://dx.doi.org/10.1063/1.4832781
7. Stange, H.; Brunken, S.; Hempel, H.; Rodriguez-Alvarez, H.; Schafer, N.; Greiner, D.; Scheu, A.; Lauche, J.; Kaufmann, C. A.; Unold, T.; Abou-Ras, D. and Mainz, R. Effect of Na presence during $CuInSe_2$ growth on stacking fault annihilation and electronic properties. *Appl. Phys. Lett.* **2015**, 107, 152103, http://dx.doi.org/10.1063/1.4933305
8. Mishra, S.; Ganguli, B. Effect of structural distortion and nature of bonding on the electronic properties of defect and Li-doped $CuInSe_2$ Chalcopyrite Semiconductors. Preprint submitted to Chemical Physics **2011**, http://arxiv.org/ftp/arxiv/papers/1103/1103.0614.pdf
9. Caballero-Briones, F.; Palacios-Padrós, A.; Calzadilla, O.; Moreira, I. de P. R.; Sanz, F. Disruption of the Chemical Environment and Electronic Structure in p-Type Cu_2O Films by Alkaline Doping. *J. Phys. Chem.* C **2012**, 116, 13524-13535, DOI: 10.1021/jp3023937
10. Economou, N. J.; Mubeen, S.; Buratto S. K. and McFarland, E. W. Investigation of Arrays of Photosynthetically Active Heterostructures Using Conductive Probe Atomic Force Microscopy. *Nano Letters* **2014**, 14, 3328−3334, DOI: 10.1021/nl500754q
11. Doron Azulay, Oded Millo, Isaac Balberg, Hans-Werner Schock, Iris Visoly-Fisher, David Cahen, Current routes in polycrystalline $CuInSe_2$ and Cu(In,Ga)Se_2 films. *Sol. Energ. Mat. Sol. Cells* **2007**, 91, 85–90, http://dx.doi.org/10.1016/j.solmat.2006.08.006
12. Tombak, A.; Benhaliliba, M.; Ocak, Y.S.; Kiliçoglu, T. The novel transparent sputtered p-type CuO thin films and Ag/p-CuO/n-Si Schottky diode applications. *RINP* **2015**, 5, 314–321, http://dx.doi.org/10.1016/j.rinp.2015.11.001
13. Arvizu-Rodríguez, L. E.; Palacios-Padrós, A.; Chalé-Lara, F.; Fernández-Muñoz, J. L.; Díez-Pérez, I.; Sanz, F.; Espinosa-Faller, F. J.; Sandoval, J.; Caballero-Briones, F. Phase and surface modification by electrochemical post deposition treatments in ultrasonic-assisted $CuInSe_2$/Cu electrodeposited films. *Chalc. Lett.* **2015**, 12, 537-545
14. Caballero-Briones, F.; Palacios-Padrós, A.; Sanz, F. $CuInSe_2$ films prepared by three step pulsed electrodeposition. Deposition mechanisms, optical and photoelectrochemical studies. *Electrochimica Acta* **2011**, 56, 9556-9567, http://dx.doi.org/10.1016/j.electacta.2011.06.024
15. Notoya, R. Kinetic studies of electron transfer step of hydrogen evolution reaction on platinum in aqueous cesium hydroxide. *J. Res. Inst. Catalysis* **1970**, 9, 17-28, http://hdl.handle.net/2115/24917
16. Oikkonen, L. E.; Ganchenkova, M. G.; Seitsonen, A. P. and Nieminen, R. M. Effect of sodium incorporation into $CuInSe_2$ from first principles. *J. Appl. Phys* **2013**, 114, 083503, http://dx.doi.org/10.1063/1.4819105
17. Elaheh Ghorbani, Janos Kiss, Hossein Mirhosseini, Guido Roma, Markus Schmidt, Johannes Windeln, Thomas D. Khune, and Claudia Felser. Hybrid-Functional Calculations on the Incorporation of Na and K Impurities into the $CuInSe_2$ and $CuIn_5Se_8$ Solar-Cell Materials. *Phys. Chem. C* **2015**, 119 (45), 25197–25203, DOI: 10.1021/acs.jpcc.5b07639
18. Rathod, K. C. Synthesis, characterization and applications of mixed chalcogenide thin films, Ph.D. Thesis, Shivaji University, India 2015, http://hdl.handle.net/10603/50673